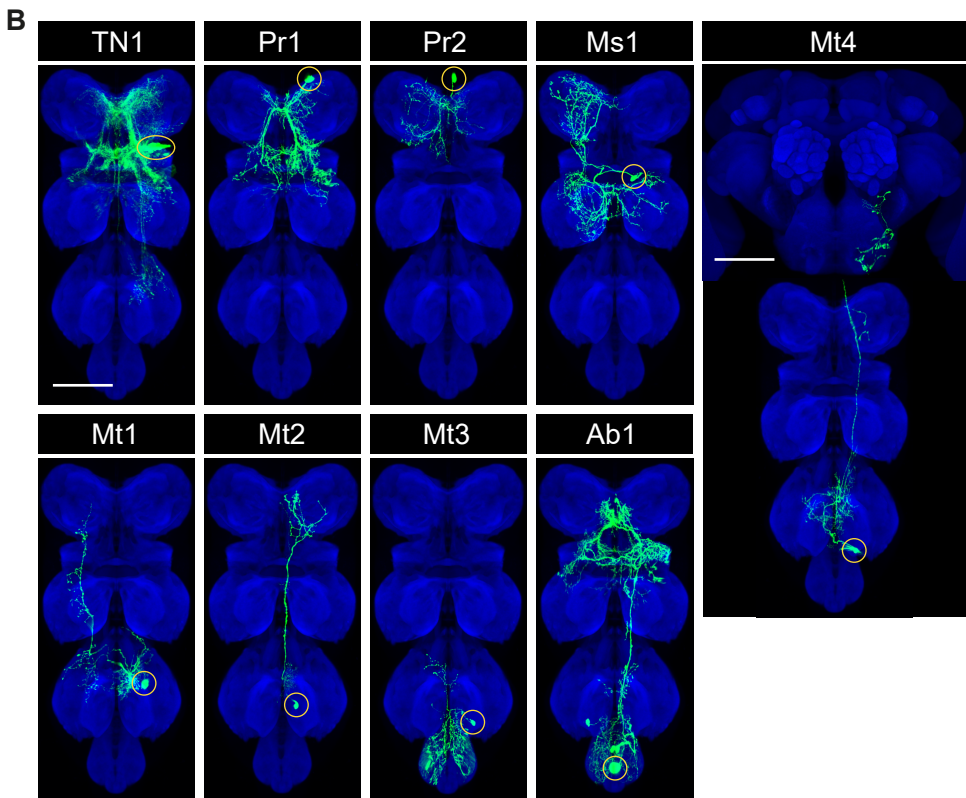
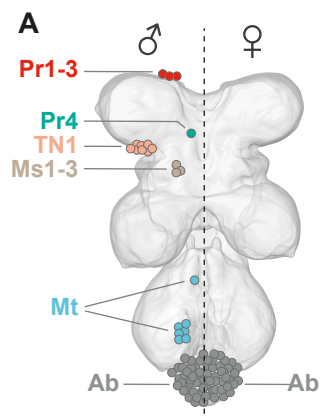


**Supplemental Information**

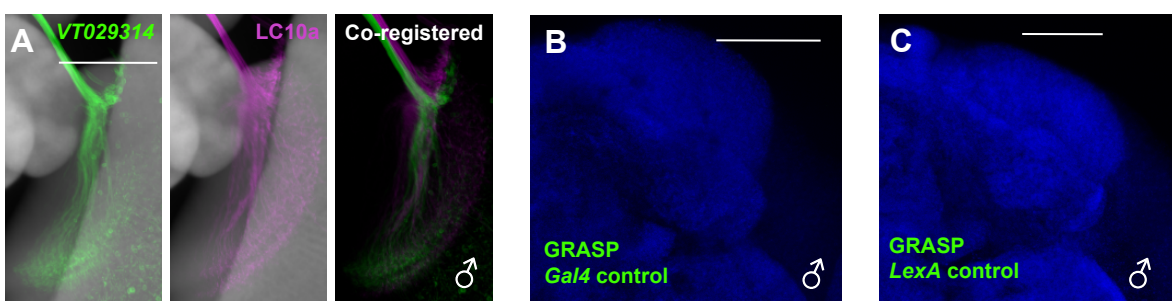
**A sex-specific switch between  
visual and olfactory inputs underlies  
adaptive sex differences in behavior**

**Tetsuya Nojima, Annika Rings, Aaron M. Allen, Nils Otto, Thomas A. Verschut, Jean-  
Christophe Billeter, Megan C. Neville, and Stephen F. Goodwin**

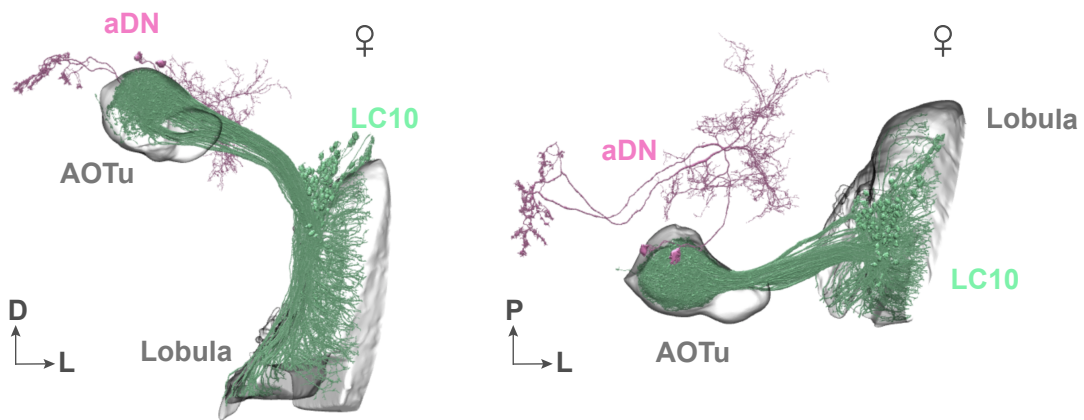


**Figure S1: Comprehensive single cluster-level mapping of *dsx*-expressing neurons in the male VNC. Related to Figure 1.**

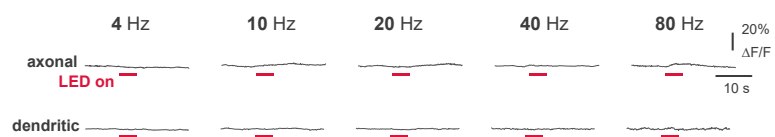
(A) A schematic drawing representing *dsx* expression pattern in the VNC. Male neurons are shown in the thoracic neuromeres on the left, the absence of female neurons is shown on the right. Neuronal differences between the sexes are not distinguished in the abdominal neuromere. (B) Male single neuroblast clones generated by *dsx<sup>Gal4</sup>*-driven MARCM. Cell body positions are indicated by yellow circles. Scale bars, 50  $\mu$ m.



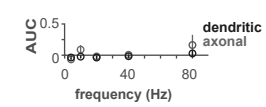
**D**



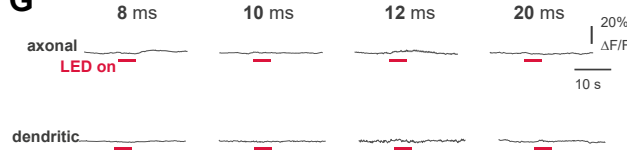
**E**



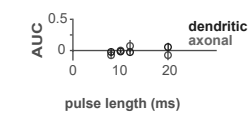
**F**



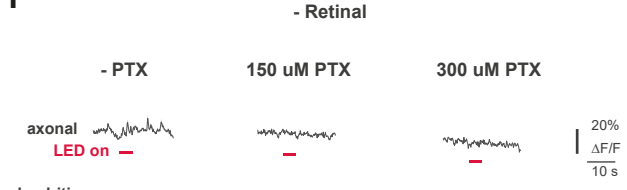
**G**



**H**



**I**



**J**

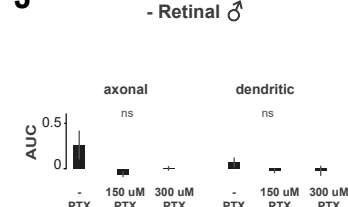


**Figure S2: Connectivity between LC10a and aDN is male-specific. Related to Figure 3.**

(A) LC10 neurons labeled by *VT029314-LexA* (green) and *OL0019B* split-*Gal4* (magenta) are co-registered (right). Scale bar, 50  $\mu$ m. (B and C) Genetic controls for the GRASP experiment either without *LexA* (B) or *Gal4* (C) driver. Scale bars, 30  $\mu$ m. (D) Positions of LC10 (green) axon terminals and aDN (magenta) dendritic fields in females are analyzed using the EM-level connectomics database neuPrint. Anterior (left) and dorsal (right) views are shown. Two neuropil regions, lobula and AOTu, which are innervated by LC10 dendrites and axons, respectively, are indicated in gray. (E) Mean (dark gray line) and standard error (SE; light gray shaded area) of  $\Delta F/F$  in aDN axonal (top) and dendritic (bottom) compartments in response to a 5 s (40 Hz, 10 ms pulses) optogenetic stimulation of LC10a neurons (pink bar) in control males not fed on all-*trans*-retinal; Left: without picrotoxin (- PTX) and CGP54626 ( $n = 13$  male); Middle: 150  $\mu$ M picrotoxin and 50  $\mu$ M CGP54626 ( $n = 8$  male flies); Right: 300  $\mu$ M picrotoxin and 50  $\mu$ M CGP54626 ( $n = 10$  and 8 male flies in axonal and dendritic compartments, respectively); (F) Mean and SE of the area under the  $\Delta F/F$  curve (AUC) from beginning until 1s after the end of the stimulus for experiments in (E). (G) Mean and SE of  $\Delta F/F$  traces in aDN axonal (top traces) and dendritic (bottom traces) compartments in response to different frequencies (4-80 Hz, 10 ms pulses) of a 5 s optogenetic activation of LC10a neurons in 9-28 males for each frequency. (H) AUC vs. frequency for data in (G) in axonal (light gray circles) and dendritic (dark gray circles) compartments. (I) Mean  $\Delta F/F$  traces in aDN axonal (top traces) and dendritic (bottom traces) compartments in response to different pulse lengths (8-20 ms, 40 Hz pulses) of a 5 s optogenetic activation of LC10a neurons in 5-28 males for each pulse length. (J) AUC vs. pulse length for data in (I). ns –  $p.adj > 0.05$  by Mann-Whitney-U test adjusted for multiple comparisons with the Holm method.

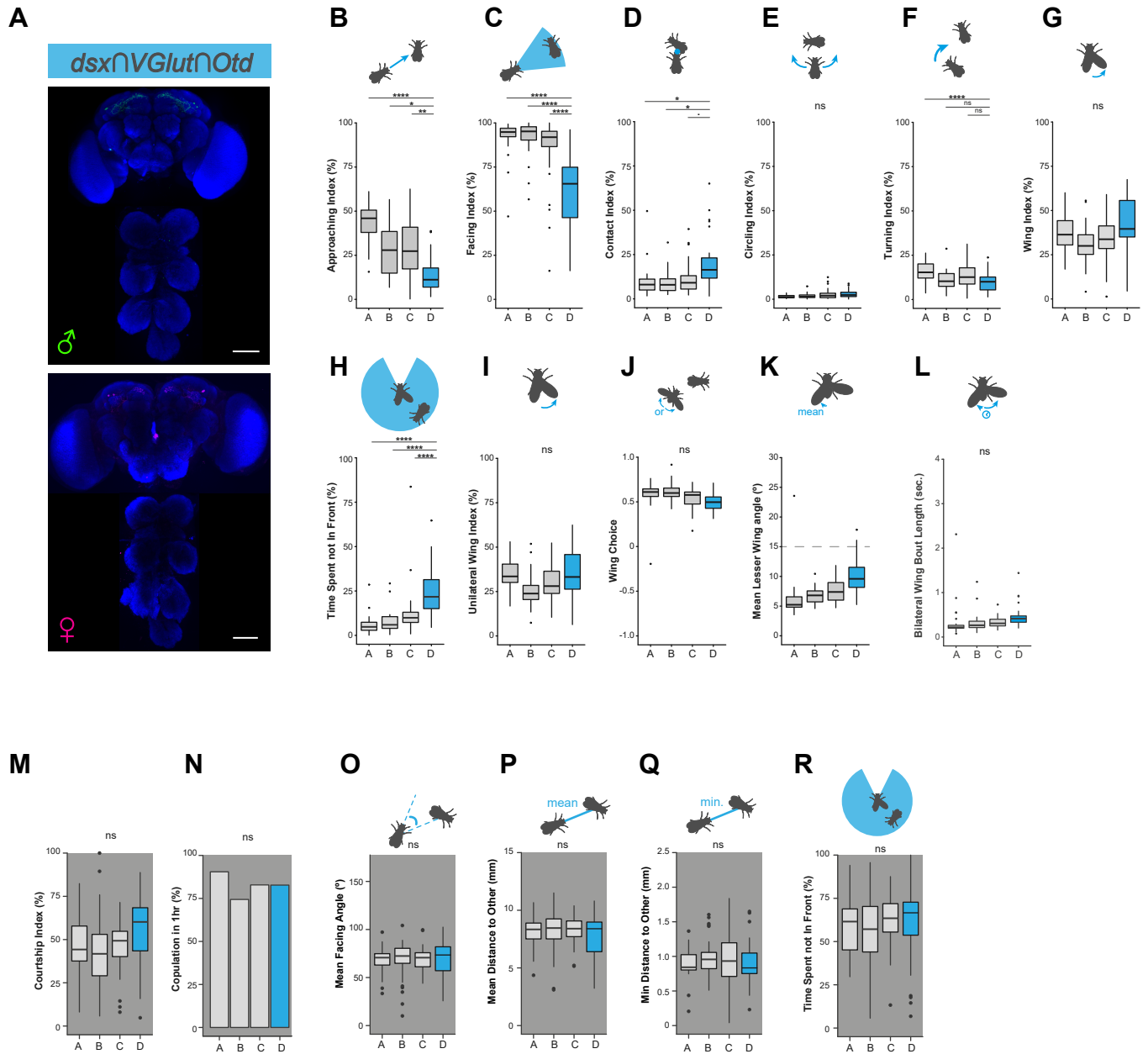


**Figure S3: Silencing male aDN alters visually guided courtship behavior. Related to Figure 4.**

**(A)** Spatially restricted expression in aDN cluster.  $dsx \cap VGlu t^{dVP16.AD} \cap Otd$  expression patterns shown using  $dsx^{Gal4.DBD}/VGlu t^{dVP16.AD}/Otd-FLP > UAS>stop>mCD8::GFP$  in the male (green) and female (magenta) brains and VNCs. Scale bar, 50  $\mu$ m. **(B-L)** Schematic representations of the behaviors are inset. **(B-F)** Individual indices of each component of courtship behavior for which a JAABA classifier was trained. The reported  $p.adj$  are  $p$  values adjusted (Holm method) for comparison of multiple behaviors. **(B)** Approaching index ( $F_{(3,114)} = 26.2$ ,  $p.adj < 0.0001$ ). **(C)** Facing index ( $F_{(3,114)} = 23.7$ ,  $p.adj < 0.0001$ ). **(D)** Contact index ( $F_{(3,114)} = 6.91$ ,  $p.adj = 0.008$ ). **(E)** Circling index ( $F_{(3,114)} = 4.11$ ,  $p.adj = 0.16$ ). **(F)** Turning index ( $F_{(3,114)} = 6.61$ ,  $p.adj = 0.011$ ). **(G)** Wing extension index. ( $F_{(3,114)} = 3.87$ ,  $p = 0.012$ ,  $p.adj = 0.19$ ). **(H)** Percent of time when the female was not in front of the male while the males wing was extended. ( $F_{(3,114)} = 28.6$ ,  $p.adj < 0.0001$ ). **(I)** Unilateral wing index. ( $F_{(3,114)} = 3.40$ ,  $p.adj = 0.32$ ). **(J)** Wing choice index. ( $F_{(3,114)} = 4.41$ ,  $p.adj = 0.11$ ). **(K)** Bilateral wing bout length. ( $F_{(3,114)} = 0.619$ ,  $p.adj = 1.0$ ). **(L)** Mean lesser wing angle. **(M)** Courtship Index (%) in the dark. ( $F_{(1,123)} = 3.143$ ,  $p.adj = 0.17$ ). **(N)** Copulation (%) over a 60-minute time period in the dark. (Fisher's exact test,  $p.adj = 1.00$ ). **(O)** Mean facing angle in the dark. ( $F_{(1,123)} = 0.173$ ,  $p.adj = 1.00$ ). **(P)** Mean distance to other in the dark. ( $F_{(1,123)} = 0.84$ ,  $p.adj = 1.00$ ). **(Q)** Minimum distance to other in the dark. ( $F_{(1,123)} = 0.453$ ,  $p.adj = 1.00$ ). **(R)** Percentage of time when the female was not in front of the male while the male's wing was extended in the dark. ( $F_{(1,123)} = 0.536$ ,  $p.adj = 1.00$ ) Full genotypes: A= $Otd-FLP/+$ ;  $dsx^{Gal4.DBD/+}$  ( $n_{light}=31$ ,  $n_{dark}=21$ ), B= $VGlu t^{dVP16.AD}$ ,  $UAS>stop>TNT/+$  ( $n_{light}=20$ ,  $n_{dark}=43$ ), C= $VGlu t^{dVP16.AD}$ ,  $UAS>stop>TNT/+$ ;  $dsx^{Gal4.DBD/+}$  ( $n_{light}=34$ ,  $n_{dark}=35$ ), D= $VGlu t^{dVP16.AD}$ ,  $UAS>stop>TNT/Otd-FLP$ ;  $dsx^{Gal4.DBD/+}$  ( $n_{light}=33$ ,  $n_{dark}=29$ ). \* $p.adj < 0.1$ , \* $p.adj < 0.05$ , \*\* $p.adj < 0.01$ , \*\*\* $p.adj < 0.001$ , \*\*\*\* $p.adj < 0.0001$  by t-test **(B-R)** and adjusted with the Holm method. ns –  $p.adj > 0.1$ .

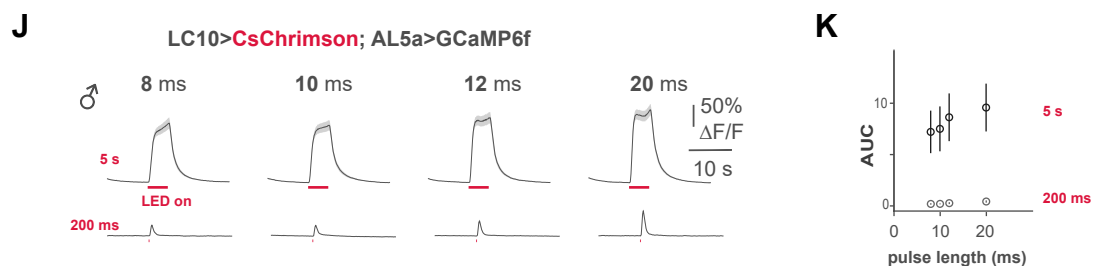
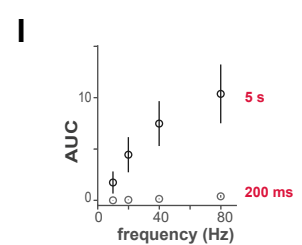
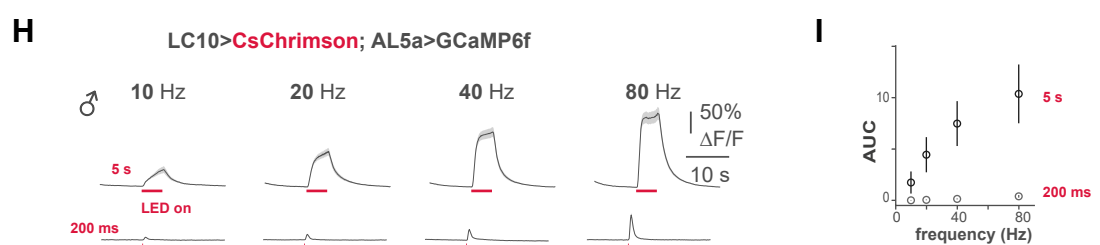
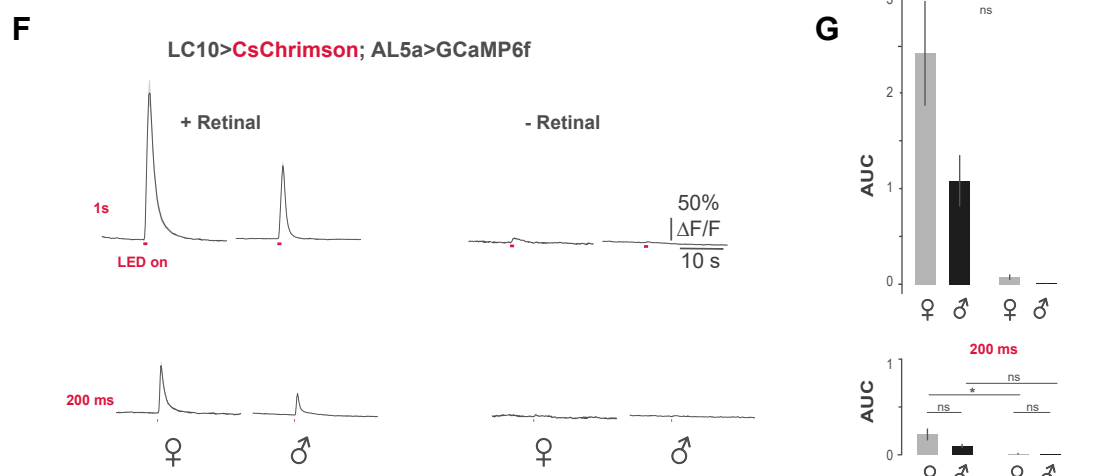
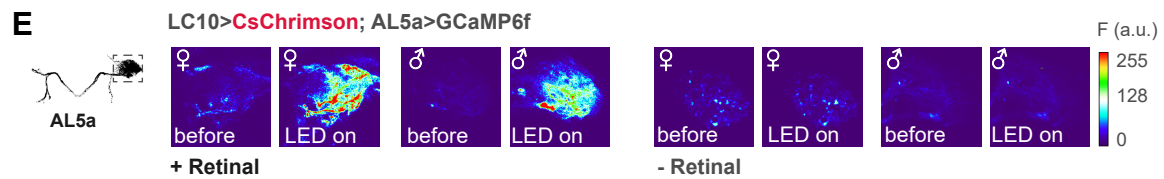
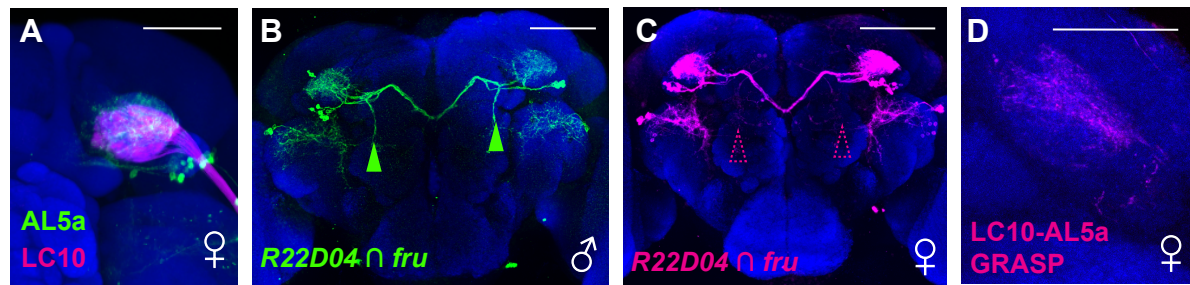


**Figure S4: *fru*-expressing AL5a is an additional downstream cluster of LC10a. Related to Figure 5.**

(A) The female LC10a (magenta) and AL5a (green) co-registered on to the template brain. Scale bar, 30  $\mu$ m. (B,C) Expression patterns of *GMR22D04-Gal4* $\cap$ *fru*<sup>FLP</sup> in the male (green) and female (magenta) brains. Solid filled (B) and dashed open (C) arrowheads indicate the presence and absence, respectively, of male-specific longitudinal neurite branches. Scale bars, 50  $\mu$ m. (D) GRASP signals between LC10a and AL5a in the female (magenta). Scale bar, 30  $\mu$ m. (E) Left: Maximum projection of a confocal stack of mCD8::GFP-labeled AL5a in a male. Recording region in the AOTu for calcium imaging is indicated by a gray box. Right: Example fluorescence recordings from the input sites of AL5a neurons in the AOTu expressing GCaMP6f in males and females before (left panel) and during (right panel) a 5 s (40 Hz, 10 ms) optogenetic stimulation of LC10a neurons expressing CsChrimson. Left (+ Retinal) Right (- Retinal). (F) Mean (dark gray) and SE (light gray shaded area) of  $\Delta F/F$  traces in AL5a neuron input sites in response to a 1 s (top) and 200 ms (bottom) optogenetic activation (pink bar, 40 Hz, 10 ms pulses) of LC10a neurons; Averages of 4 pulses each in retinal fed (+Retinal, left) female (left, n=7) and male (right, n=11) flies and in non-retinal control (-Retinal, right) female (left, n=8) and male (right, n=7) flies. (G) Mean and SE of AUC for experiments in (F); Top: 1 s optogenetic stimulation; Bottom: 200 ms optogenetic stimulation. (H) Mean  $\Delta F/F$  traces in AL5a neurons in response to different frequencies (10 - 80 Hz, 10 ms pulses) of a 5 s (top) and 200 ms (bottom) optogenetic activation of LC10a in n = 11-13 males for each frequency. (I) Mean and SE of AUC for experiments in (H) for 5 s (dark gray circles) and 200 ms (light gray circles) optogenetic stimulation of LC10a. (J) Mean  $\Delta F/F$  traces in AL5a neurons in response to different pulse lengths (8 - 20 ms, 40 Hz pulses) of a 5 s (top) and 200 ms (bottom) optogenetic activation of LC10a in 10 -13 males for each pulse length. (K) Mean and SE of AUC for experiments in (J) for 5 s (dark gray circles) and 200 ms (light gray circles) optogenetic stimulation of LC10a. ns –  $p.adj > 0.05$ , \* $p.adj < 0.05$ , \*\* $p.adj < 0.01$ , \*\*\* $p.adj < 0.001$ , \*\*\*\* $p.adj < 0.0001$  by Mann-Whitney-U test adjusted for multiple comparisons with the Holm method.

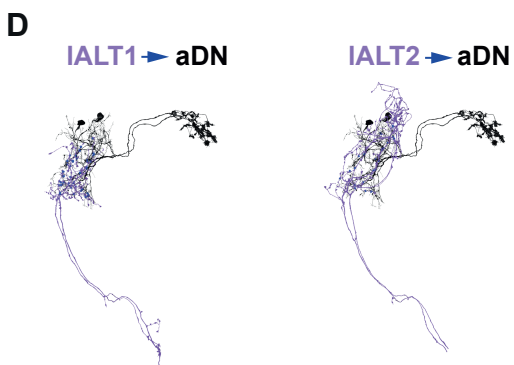
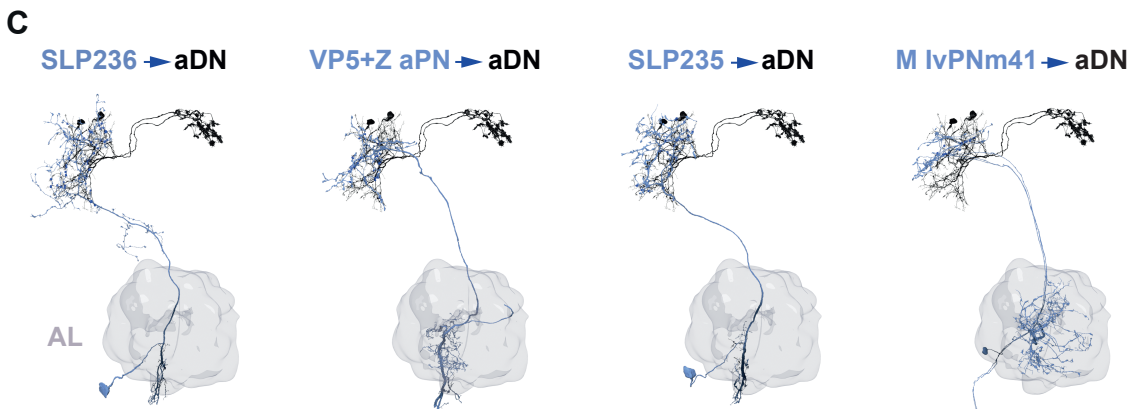
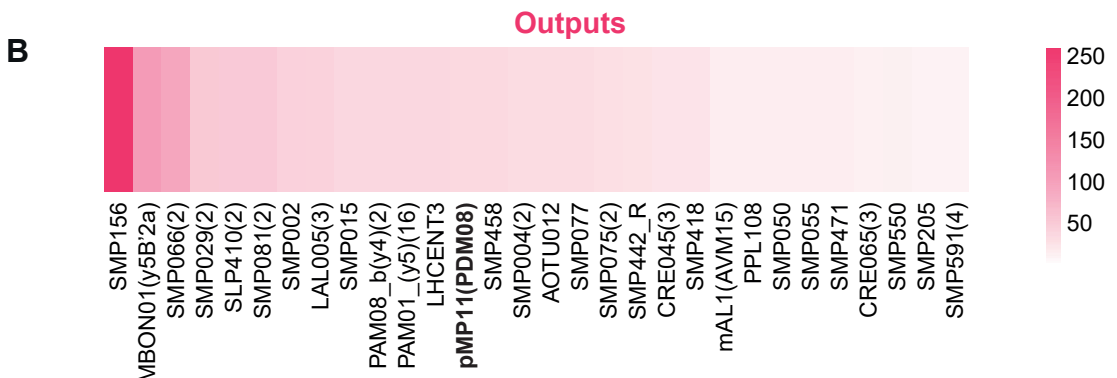
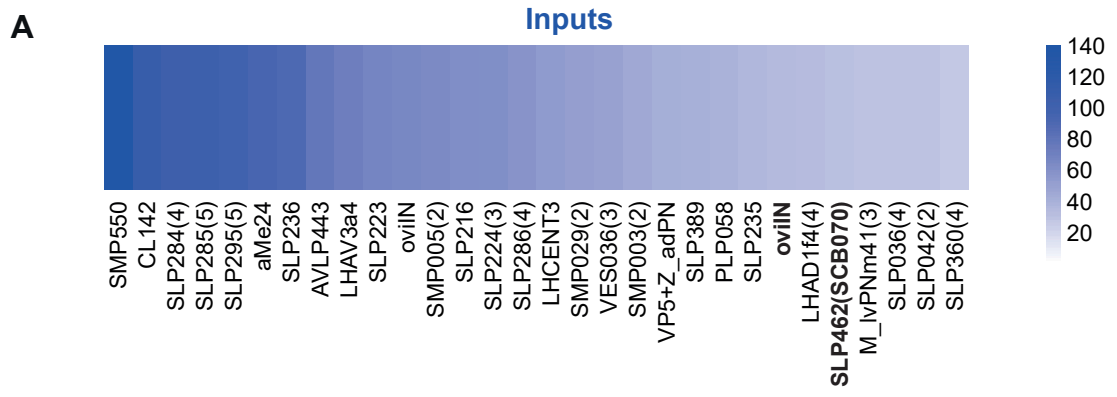


**Figure S5: Female aDN connectivity. Related to Figure 6.**

**(A and B)** Heatmaps representing number of synaptic connections to both aDN combined input (**A**) and output (**B**) by neuronal types. Neurons labeled in bold are contralateral, all others are ipsilateral. Color scales represent the number of synapses. **(C and D)** 3D reconstructions of volumetric EM data of aDN (2 neurons, grey) and projection neurons in the right-brain hemisphere. **(C)** The multiglomerular multimodal projection neurons VP5+Z aPN (bodyid: 5813063239) and M LvPNm41 (bodyids: 730252777, 1765415970, 1795410644) are shown as well as the uncharacterized non-olfactory projection neurons SLP236 (bodyid: 420274150) and SLP235 (5813056890). Inputs into the aDN are shown in blue. The antennal lobe (AL) is shown. **(D)** The IALT-tract neurons classes IALT1 (bodyid: 888500672) and IALT2 (bodyid: 5901195362) are shown.

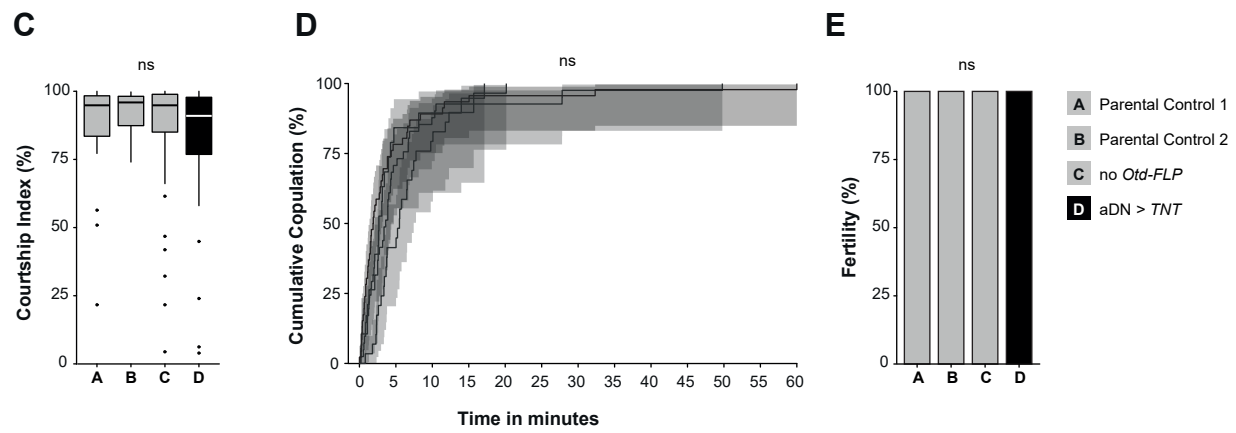
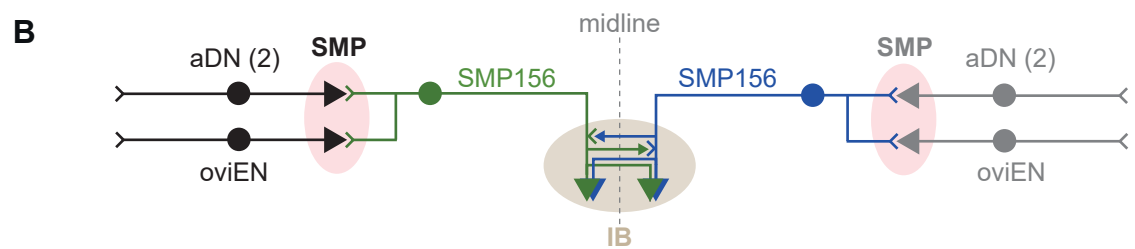
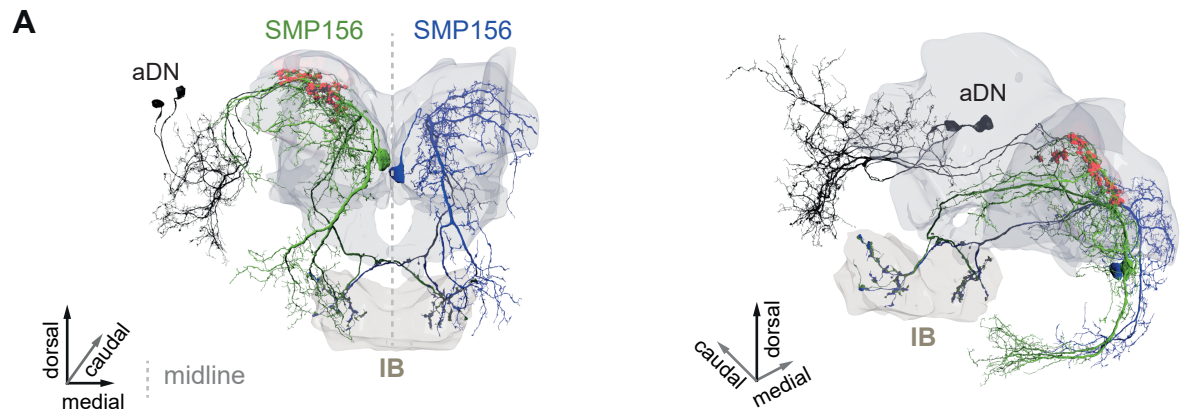


**Figure S6: Female aDNs are not involved in virgin female behavior. Related to Figure 7.**

**(A)** 3D reconstructions of volumetric EM data from aDN (2 neurons, grey) and the contra- and ipsilateral downstream neurons SMP156 (bodyids: 5813022337, 673776769). The inferior bridge (IB) and the SMP for both hemispheres are shown as well. Synapses from aDN to SMP156 are shown in red. **(B)** Circuit diagram shows aDN and oviEN inputs to SMP156 that projects to the IB. **(C-E)** Silenced female aDN behaviors (ns –  $p.adj > 0.05$ ). **(C)** Control male courtship indices toward female. ( $F_{(3,131)} = 1.1$ ,  $p = 0.49$ ,  $p.adj = 1$ ). **(D)** Cumulative proportional copulation (%  $\pm$  95% confidence intervals) over a 60-minute time period. ( $\chi^2_{(3)} = 5.5$ ,  $p = 0.14$ ,  $p.adj = 1$ ). **(E)** Individual female fertility over a 1-week period. (Fisher's Exact Test,  $p = 1$ ).

	<b>Male</b>	<b>Female</b>
	Mean ± SEM (n)	Mean ± SEM (n)
<b>pC1</b>	$48 \pm 3.1$ (10)	$6 \pm 0.3$ (8)
<b>pC2m</b>	31 (1)	NA
<b>pC2l</b>	$44 \pm 2.4$ (10)	$13 \pm 0.5$ (7)
<b>pCd-1</b>	15 (2)	$8 \pm 1.1$ (2)
<b>pCd-2</b>	3 (10)	3 (10)
<b>pMN1</b>	NA	NA
<b>pMN2</b>	NA	1 (10)
<b>pMN3</b>	1 (10)	NA
<b>pLN</b>	1 (10)	NA
<b>aDN</b>	2 (10)	2 (10)
<b>SN</b>	1 (10)	NA
 <b>TN1</b>	$24 \pm 0.8$ (6)	NA
<b>Pr1</b>	1 (3)	NA
<b>Pr2</b>	1 (1)	NA
<b>Ms1</b>	1 (1)	NA
<b>Mt1</b>	1 (1)	NA
<b>Mt2</b>	1 (1)	NA
<b>Mt3</b>	1 (1)	NA
<b>Mt4</b>	1 (1)	NA
<b>Ab1</b>	1 (1)	NA

**Table S1. Numbers of cells in *dsx*<sup>+</sup> single clusters. Related to Figure 1.**

Figure	Full genotype
1C-1E, S1B	<i>y, w, hs-flp(22); FRTG13, UAS-mCD8::GFP/FRTG13, tubP-Gal80; dsx<sup>Gal4</sup>/UAS-mCD8::GFP</i>
1C, 2A-2C, 2E-2G, 3B	<i>10xUAS-IVS-mCD8::GFP/VGlu<sup>dVP16.AD</sup>; dsx<sup>Gal4.DBD</sup>/+</i>
1D	<i>10xUAS-IVS-mCD8::GFP/+; dsx<sup>Gal4.DBD</sup>/Trh-p65.AD</i>
2I-2K	<i>UAS-DenMark/VGlu<sup>dVP16.AD</sup>; dsx<sup>Gal4.DBD</sup>/+</i>
2L-2N	<i>UAS-Syb::GFP/VGlu<sup>dVP16.AD</sup>; dsx<sup>Gal4.DBD</sup>/+</i>
3A-3B, 5B-5C, S2A, S4A	<i>R35D04-p65.AD/10xUAS-IVS-mCD8::GFP; R22D06-Gal4.DBD/+</i>
3D-3G	<i>VGlu<sup>dVP16.AD</sup>/VT029314-LexA; dsx<sup>Gal4.DBD</sup>/UAS-CD4::spGFP1-10, lexAop-CD4::spGFP11</i>
3H-3I, S2E-S2J	<i>lexAop-CsChrimson::tdTomato, UAS-GCaMP6f/+; VGlu<sup>dVP16.AD</sup>/VT029314-LexA; dsx<sup>Gal4.DBD</sup>/+</i>
4, 7E-7G, S3B-S3R, S6C-S6E	<i>Otd-FLP/+; dsx<sup>Gal4.DBD</sup>/+</i>
4, 7E-7G, S3B-S3R, S6C-S6E	<i>VGlu<sup>dVP16.AD</sup>, UAS&gt;stop&gt;TNT/+</i>
4, 7E-7G, S3B-S3R, S6C-S6E	<i>VGlu<sup>dVP16.AD</sup>, UAS&gt;stop&gt;TNT/+; dsx<sup>Gal4.DBD</sup>/+</i>
4, 7E-7G, S3B-S3R, S6C-S6E	<i>VGlu<sup>dVP16.AD</sup>, UAS&gt;stop&gt;TNT/Otd-FLP; dsx<sup>Gal4.DBD</sup>/+</i>
5A-5C	<i>y, hs-flp; FRTG13, UAS-mCD8::GFP/FRTG13, tubP-Gal80; fru<sup>NP21</sup>/UAS-mCD8::GFP</i>
5D-5E, S4A	<i>UAS-DenMark/+; GMR22D04-Gal4/+</i>
5F, S4D	<i>VT029314-LexA/+; GMR22D04-Gal4/UAS-CD4::spGFP1-10, lexAop-CD4::spGFP11</i>
5G-5H, S4E-S4K	<i>lexAop-CsChrimson::tdTomato, UAS-GCaMP6f/+; VT029314-LexA/+; GMR22D04-Gal4/+</i>
6F-6G	<i>lexAop-CsChrimson::tdTomato, UAS-GCaMP6f/+; VGlu<sup>dVP16.AD</sup>/GH146-LexA; dsx<sup>Gal4.DBD</sup>/+</i>
6H-6I	<i>lexAop-CsChrimson::tdTomato, UAS-GCaMP6f/+; VGlu<sup>dVP16.AD</sup>/+; dsx<sup>Gal4.DBD</sup>/Orco-LexA::VP16</i>
S2A	<i>VT029314-LexA/13xlexAop2-IVS-myrl::GFP</i>
S2B	<i>VGlu<sup>dVP16.AD</sup>/+; dsx<sup>Gal4.DBD</sup>/UAS-CD4-spGFP1-10, lexAop-CD4-spGFP11</i>
S2C	<i>VT029314-LexA/+; UAS-CD4-spGFP1-10, lexAop-CD4-spGFP11/+</i>
S3A	<i>VGlu<sup>dVP16.AD</sup>/Otd-FLP; dsx<sup>Gal4.DBD</sup>/UAS&gt;stop&gt;mCD8::GFP</i>
S4B-S4C	<i>UAS&gt;stop&gt;mCD8::GFP/+; GMR22D04-Gal4/fru<sup>FLP</sup></i>

**Table S3. Full genotype list. Related to Figures 1-7 and Figures S1-S4, S6.**